# Mechanical and Antimicrobial Properties of Multilayer Films with a Polyethylene/Silver Nanocomposite Layer

**S. Sánchez-Valdes,[1] H. Ortega-Ortiz,[1] L. F. Ramos-de Valle,[1] F. J. Medellín-Rodríguez,[2] R. Guedea-Miranda[1]**

[1]*Centro de Investigación en Química Aplicada (CIQA), Departamento de Procesos de Transformación, Saltillo, Coahuila 25253, México*
[2]*Centro de Investigación y Estudios de Posgrado/FCQ/UASLP, Departamento de Ingeniería Química, Av. Dr. Manuel Nava 6 Zona Universitaria, San Luis Potosi 78210, México*

Received 12 December 2007; accepted 6 July 2008
DOI 10.1002/app.29051
Published online 17 October 2008 in Wiley InterScience (www.interscience.wiley.com).

**ABSTRACT:** A layer of a polyethylene–silver nanoparticles composite was deposited on a five layer barrier film structure. Different methods were used for the nanocomposite layer deposition: laminating, casting, and spraying over the multilayer structure. For the casting and spraying methods, the silver nanoparticles were previously dispersed in the polymer solution, with the assistance of ultrasound energy. The effect of silver nanoparticles and deposition method on the barrier, mechanical, and optical properties of the multilayer films was evaluated. The efficiency of silver ion release from the PE-Silver nanocomposite deposited on the multilayer films and their antimicrobial characteristics were investigated and discussed. The silver ion release and biocide effect of the multilayer films was found to be dependant on the silver nanoparticle content and on the deposition method used. The observed results could be helpful in the design of industrial films for packaging. © 2008 Wiley Periodicals, Inc. J Appl Polym Sci 111: 953–962, 2009

**Key words:** multilayered films; silver nanoparticles; packaging films; antimicrobial properties

## INTRODUCTION

Nanocomposites are a novel class of composite materials that have received special attention because of their improved properties at very low loading levels compared with conventional filler composites. Among these improved properties are mechanical, dimensional, barrier to different gases, thermal stability, and flame retardant enhancements with respect to the bulk polymer.[1–5]

During the last few years, the spread of emerging infectious diseases, especially those caused by drug-resistant pathogens, has become a growing global concern.[6] Polymeric materials play an important role in the transmission of infections because microorganisms often have strong abilities to survive on ordinary polymeric materials, making the polymers a potential source of contamination.[7,8] The development of biocidal polymers, that is, polymers that can inactivate infectious pathogens upon contact, has attracted considerable research interest.[9–16]

Recently, silver-based antimicrobial materials have attracted significant interest.[17–21] Metallic silver is considered to be a nonreactive material, but it has been demonstrated that in aqueous environments, it can release silver ions and inhibit the microbial activity.[22]

Silver has been used as an additive in various polymers[23–25] to generate antimicrobial properties. Some silver-containing fillers commercially available, such as zirconium phosphate or titanium dioxide, as well as some zeolites have been used as silver carriers. Silver-substituted zeolites are one of the most widely used antimicrobial additives in food packaging materials. Sodium ions present in zeolites are substituted by silver ions. These zeolites have been incorporated into many commercial polymers, such as polypropylene, polyethylene (PE), and polyamide, commonly at levels of around 1–5%.[26]

Some examples of silver applications are the inorganic composites with a slow silver release rate that are currently used as preservatives in a variety of products; another current application includes compounds composed of silica gel microspheres, which contain a silver thiosulfate complex, that are mixed into plastics for long-lasting antibacterial protection.[27] Silver compounds have also been used in the medical field to treat burns and a variety of infections.[28]

The bactericidal effect of silver ions on microorganisms is very well known; however, the bactericidal mechanism is only partially understood. It has been

*Correspondence to:* S. Sánchez-Valdes (saul@ciqa.mx).
Contract grant sponsor: Mexican National Council for Science and Technology (CONACYT); contract grant number: SEP-2007-C-60962.

proposed that ionic silver strongly interacts with thiol groups of vital enzymes and inactivates them.[29,30] The silver ions avidly bind to negatively charged components in proteins and nucleic acids, thereby causing structural changes in bacterial cell walls, membranes, and nucleic acids that affect viability.[31] In particular, silver ions are thought to interact with a number of functional groups; a few of them have been identified as thiol groups, carboxylates, phosphates, hydroxyls, imidazoles, indoles, and amines.[32] Hence, silver ions that bind to DNA block transcription, and those that bind to cell surface components interrupt bacterial respiration and adenosine triphosphate (ATP) synthesis.[33] Experimental evidence suggests that DNA loses its replication ability once the bacteria have been treated with silver ions.[28] Other studies have shown evidence of structural changes in the cell membrane as well as the formation of small electron-dense granules formed by silver and sulfur.[28,34]

It has been demonstrated that the prolonged and steady release of silver ions, and hence the antimicrobial properties, are enhanced in an aqueous environment. Hence, water diffusion characteristics of the silver composites system are important parameters of the antimicrobial properties. The filler can improve the water permeation characteristics of composites either by reducing the polymer crystallinity[35] or by generating more free voids within the specimen to allow the entry of more water molecules. The silver ion release from the composites depends on the polarity of the matrix that affects water uptake, crystallinity, and the presence of certain fillers that can improve the water diffusion.[25]

Silver ions have been demonstrated to be useful and effective in bactericidal applications, but because of the unique properties of nanoparticles, nanotechnology presents a reasonable alternative for the development of new bactericides. There are several reports on multilayer films containing nano silver via layer by layer assembly of a chitosan-silver complex with antimicrobial activity but mainly focused to medical applications.[36–39]

This work reports mainly the silver ion release capability of PE nanocomposites deposited by several methods on a multilayer film structure. A comparison of their silver ion release efficacies and antimicrobial properties, at different periods, is discussed. The effect of silver nanoparticles and deposition method on barrier, mechanical, and optical properties of the multilayered films was also discussed.

## EXPERIMENTAL

### Materials

The polymers used for the preparation of the multilayer film were linear low density polyethylene (LLDPE, Dowlex 2045), supplied by Dow chemical with a melt index of 1.0 g/10 min, a graft copolymer of maleic anhydride onto polyethylene (PE-*g*-MA), Bynel 4107 from Du Pont, and a polycaprolactam (PA6), Ultramid B4 from BASF with a melt index of 17.5 g/10 min. Prior to processing, PA6 was dried in a vacuum oven for 10 h at 85°C.

Nanotechnologies, Inc. synthesized elemental silver nanoparticles used in this work. The final product is a powder of foamy carbon-coated silver nanoparticles that were used without further treatment. These nanoparticles are embedded in a foamy carbon matrix, which prevents coalescence during their synthesis. These nanoparticles have an average size of 25 nm and a specific surface area (SSA) of 23 $m^2/g$. The interactions between the silver nanoparticles and the foamy carbon-matrix are very weak so that the nanoparticles need very low energy to be released from this carbon matrix.

### Preparation of the multilayer film

The five layer film used as a substrate was prepared by coextruding PE as the external layers with PA6 as the central layer and PE-*g*-MA as tie layers, in a five-layer 75 ± 2 μm thick flat film: PE/tie/PA6/tie/PE, using three-single-screw extruders (L/D = 24, KTS-100 from Davis Standard, USA) connected to a multilayer feed block fitted with a flat die, with temperature of 250°C at the die. Seventy seven weight percent of this film was PE, 17% PA6, and 6% adhesive. The five layer film was used as a substrate to study the effect of the silver nanoparticles directly on a multilayer structure similar to those used in the packaging industry.

A thin layer, around 10 ± 2 μm, of the silver-PE nanocomposite was deposited over the described five-layer film by different methods:

#### Laminating method

The silver-PE nanocomposite was melt blended in a 300-$cm^3$ mixing chamber, coupled to a Brabender Torque Rheometer (Brabender PL-2000, USA), with nitrogen flux, preheated to 150°C, using two sigma rotors at a roller speed of 60 rpm. The silver nanocomposite was laminated at the desired silver content by extrusion and melt cast to form a layer of around 10 ± 2 μm over the five-layer film substrate. This is called the laminating method.

#### Casting method

A homogenous suspension of specific silver nanoparticle content in a solution of PE and xylene at 120°C was obtained with and without the assistance

of a Sonicator ultrasonic processor (Industronic AMCR-5118, Mexico).

A probe of ultrasonic oscillation with a maximum power output of 300 W and a frequency of 20 kHz was used for the homogeneous dispersion of the silver nanoparticles in the polymer solution. This nanocomposite suspension was deposited by solution casting, forming a layer of around 10 ± 2 μm over the previously described five-layer structure. All the samples were vacuum dried at near 80°C for 8 h to evaporate the remaining solvent. The deposition process was controlled trying to obtain the desired and most homogeneous thickness controlling the amount of deposited nanocomposite suspension. This is called the casting method.

### Spraying method

This nanocomposite suspension was also deposited by spraying, using a metallic sprayer to form a layer of around 10 ± 2 μm over the five-layer film structure. All the samples were vacuum dried at near 80°C for 8 h to evaporate the remaining solvent. Controlling the number of sprayed layers, it was possible to obtain the desired and most homogeneous thickness. This is called the spraying method.

### Characterization of multilayer films

The mechanical properties of the resulting multilayer films were measured according to ASTM D 882 with an Instron Model 4301, USA. UV–visible spectroscopy (HP 8452 spectrophotometer, USA) was used to determine the optical properties of the silver nanocomposites. Light transmission and haze were determined according to ASTM D1003, using a Hazegard Plus from BYK Gardner, USA. Film surfaces of average specimens were analyzed by scanning electron microscope (SEM), Model Top Con 510 SM, USA. The TEM observations were performed for the thin sections of thin films with a Jeol-2000EX microscope (Jeol, USA) with a field emission gun at an accelerating voltage of 200 kV. The average nano silver particle distribution was calculated from the TEM images using an image analyzer software "Image Plus." The oxygen barrier properties were evaluated in films according to ASTM D3985 using 100% oxygen in an Oxtran 2/20-MH from MOCON, USA. Water vapor transmission was determined at 38°C and 90% relative humidity (R.H.) according to ASTM R-96 in a Permatran W 3/31 MA, PERMATRAN, USA. Reported permeability results are the average of at least six specimens per sample.

To monitor the silver ion release and antimicrobial characteristics, the composites were stored in bottles containing water (distilled and deionized) and continuously shaken. The analytes collected under these conditions were used for the experiments to quantify the silver ion released by the composites at various time intervals using an IPC spectrophotometer Thermo Jarrel ASH, Advantage, USA.

The antimicrobial tests were performed by using ASTM E 2149-01 method. The samples were tested against microorganisms supplied by American Type Culture Collection (ATCC) a bacteria *Pseudomonas oleovorans* (ATCC 29347) and a fungus *Aspergillus níger* (ATCC 6275). The strains were grown and multiplied in peptone–agar and PDA media at 30 and 28°C, respectively.

The test was made by inoculating the bacteria *P. oleovorans* in peptone–agar and the *A. niger* in PDA, then a film of 2.5 cm diameter previously sterilized with ethanol was placed in a Petri dish that was immediately incubated at an optimum temperature for 24 h for *P. oleovorans* and 72 h for *A. niger*. After this period of time, the samples were visually analyzed (qualitatively) for the inhibition of bacteria and fungi growth. Three replications were maintained for every treatment of this study.

For the test in media broth, an autoclave (Tuttnauer BRINKMANN 2540E) at 121°C for 15 min was used for sterilization process. The films formulated with silver nanoparticles were sterilized with ethanol. For all the strains, a concentration of $10^6$ CFU/mL was used in the antimicrobial assays in this study. The antimicrobial activity was evaluated by inoculating *P. oleovorans* in peptone broth (30°C) and *A. niger* in potato–dextrose broth (28°C), followed by the addition of each one of the films. The flasks were then immediately incubated in a rotary shaker (at 150 rpm) at an optimum temperature for 24 h for *P. oleovorans*, and the samples were withdrawn at 3 h intervals to check for bacterial growth. Five replications were carried out for every treatment of this study.

In the case of *A. niger*, the flasks were incubated for 72 h and the samples were withdrawn at 24 h intervals to check the fungi growth. Five replications were carried out for every treatment of this study. In all the cases, a control sample (media broth) and a reference multilayer film without silver nanoparticles were tested as reference samples.

The growth of bacterial strains was measured by determining the total proteins (biomass production) using the Peterson method at 750 nm in a UV–vis spectrophotometer (GENESYS; Model 10UV, USA).

The inhibition percentage (%) was evaluated by comparing the count of biomass (mg/mL) between the tests and control sets after 24 h of incubation for bacteria and after 72 h for the fungi.

## RESULTS AND DISCUSSION

Figures 1 and 2 present the TEM images and the silver particle size distributions of the cast thin layer of

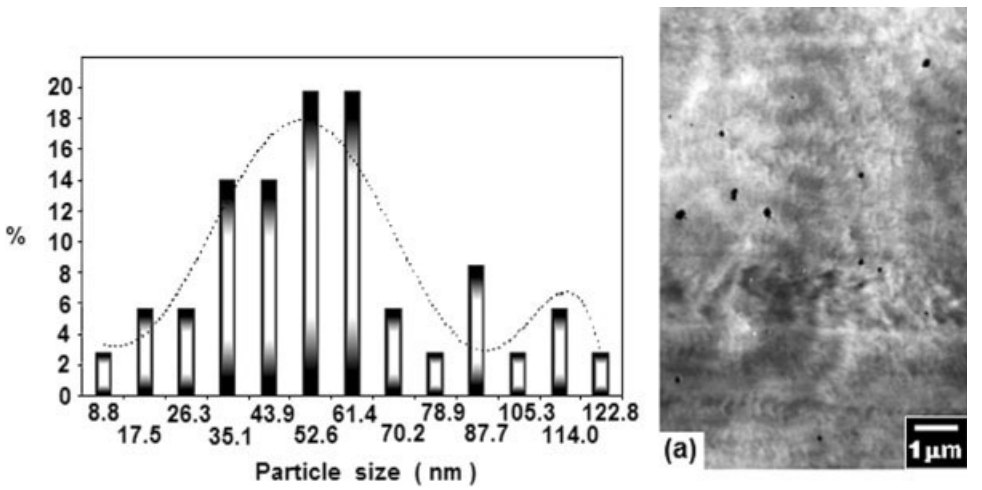


**Figure 1** TEM image and particle size distribution of the multilayer sample with a cast thin layer of PE-silver nanocomposite (0.6 wt % of silver), prepared without using ultrasonic irradiation.

the PE-silver nanocomposite prepared with and without the assistance of ultrasonic irradiation. It can be seen in both figures that the silver nanoparticles had spherical shapes and that the ultrasonic irradiation had a significant effect on the particle size dispersion. In Figure 1, the sample without ultrasonic irradiation shows silver particle aggregates of more than 100 nm and a broad size distribution with an average size between 50 and 60 nm. On the other hand, the sample shown in Figure 2, in which ultrasonic irradiation was used, showed smaller particles with an average particle size around 26 nm, less particle aggregates and a more homogenous particle size distribution. This suggests that the ultrasonic oscillations improve the dispersion of silver nanoparticles in PE matrix by exposing them to alternate compression and expansion modes of the fluid that would fragment the silver agglomerates.[40] These results are in agreement with those reported by several authors that ultrasound could disperse nanoclay uniformly as well as improve the direct dispersion of fillers during melt mixing.[41–44]

UV–visible spectroscopy is a valuable tool for structural characterization of silver nanoparticles. It is well known that the optical absorption spectra of metal nanoparticles are dominated by surface plasmon resonances (SPR), which shift to longer wavelengths with increasing particle size.[45] In general, the number of SPR peaks decrease as the symmetry of the nanoparticle increases[46] and the SPR peak wavelength increases with particle size.

Figure 3 presents UV–vis spectra of the multilayer sample with a cast thin layer of PE-silver nanocomposite at different silver contents. The sample with 0.4 wt % of nano silver exhibited the value of λ max at the lowest wavelength (370 nm) indicating that at

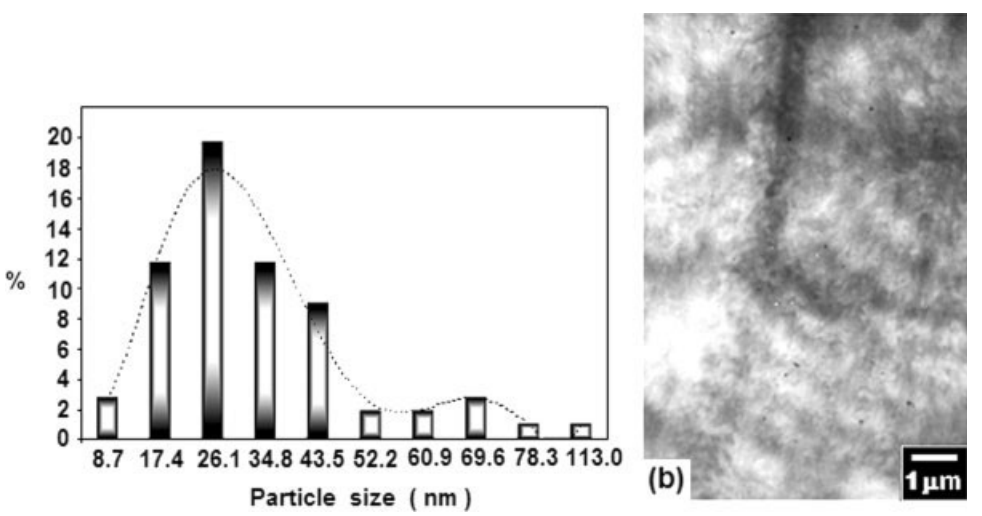


**Figure 2** TEM image and particle size distribution of the multilayer sample with a cast thin layer of PE-silver nanocomposite (0.6 wt % of silver), prepared using ultrasonic irradiation.

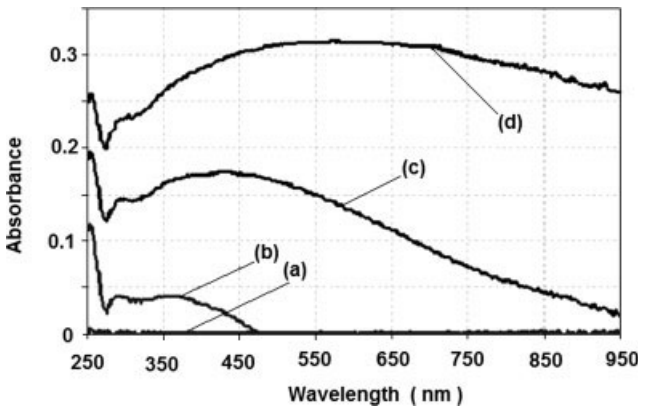


**Figure 3** UV–visible spectrum of the multilayer sample with a cast thin layer of PE-silver nanocomposites at different silver contents: (a) Reference film, (b) 0.4 wt %, (c) 0.6 wt %, (d) 1.0 wt %.

this silver content the Ag particle size was the smallest. The samples with higher nano silver particle contents show a shift in the value of λ max to higher wavelengths (440 and 560 nm), which suggests an increase in the degree of nanoparticle aggregation at these contents. This suggests that at higher contents, there is a tendency of the particles to form aggregates. Although some aggregation occurred as a result of the very small particle size, the antimicrobial properties remained, as will be seen later.

Figure 4(a–d) shows the SEM micrographs of the multilayer sample surfaces with the layer of PE-silver nanocomposite deposited by different methods. The reference multilayer film without the silver nanocomposite extra layer [Fig. 4(a)] shows a very smooth surface, whereas the sample with the nanocomposite layer deposited by lamination [Fig. 4(b)] shows a bit rough surface, in which only a few silver nanoparticle aggregates can be observed. The samples in which the silver nanocomposite was deposited by casting [Fig. 4(c)] show a much rougher surface with a few tiny pores, and it is possible to see few dispersed aggregates of silver particles. This surface roughness is caused by the solvent evaporation. The formation of these silver aggregates may be attributed to the very small silver particle size that forms aggregates when the solvent is evaporating. The sample in which the silver nanocomposite was deposited by spraying [Fig. 4(d)] shows also a very rough surface with more visible tiny pores and with more visible and dispersed silver particles on the surface. These tiny pores observed in the casting and spraying methods could permit the entry of water molecules into the composites and enhance the microbial activity of the silver particles. These pores are inherent channels that may facilitate the diffusion and migration of the chemical entities within the matrix. It can be surmised that the thin silver nanocomposite layer application method has

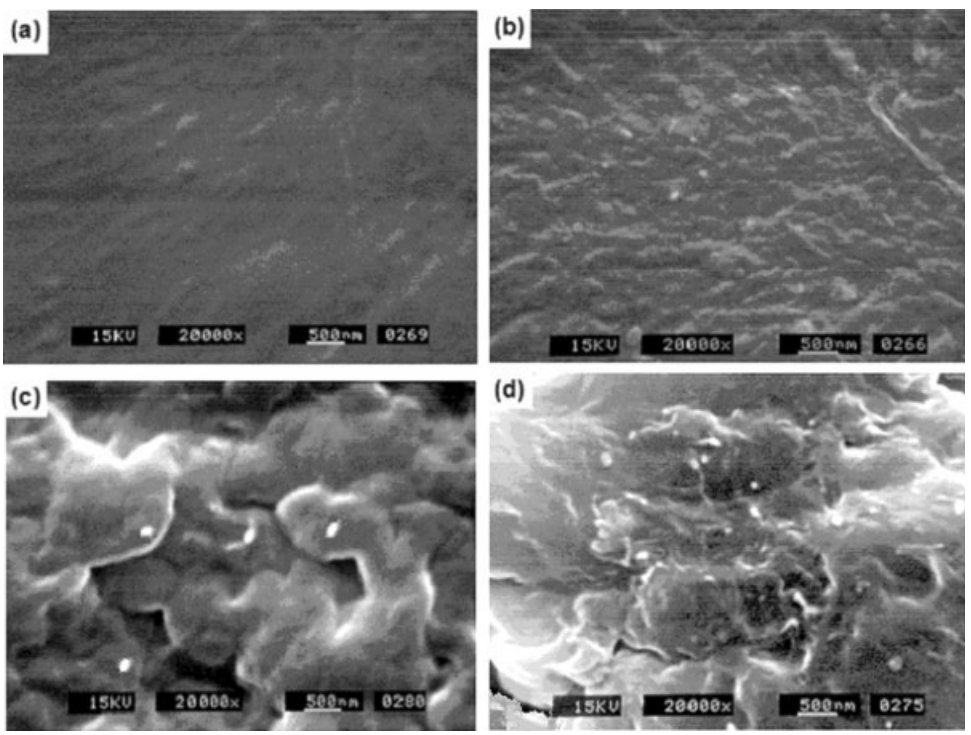


**Figure 4** SEM micrographs of surfaces of: (a) multilayer reference film, (b) laminating method, (c) casting method, and (d) spraying method.

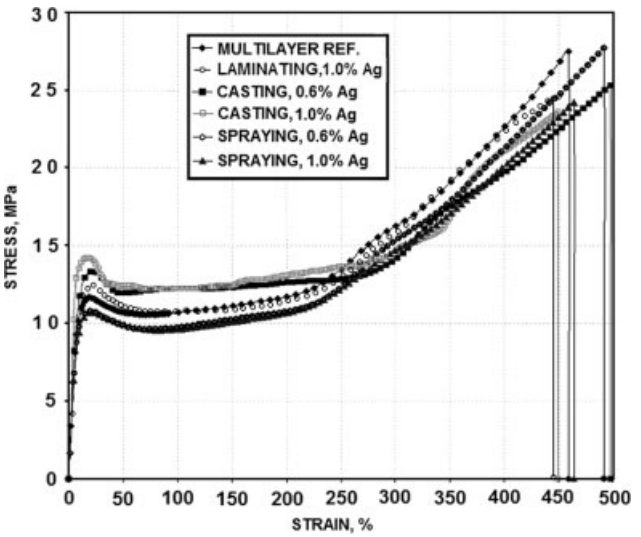


**Figure 5** Strain–stress behavior for the multilayer films.

an influence on the surface topography of the multilayer film.

Figure 5 exhibits the strain–stress behavior for the multilayer films. It can be seen that all films show a well-defined yield point. After this point, a minimum value of stress is attained, while necking is occurring, characteristic of the PA6 polymer, and then an increase in strain as the stress increases until the sample breaks, characteristic of PE polymers. The same behavior can be seen in all the samples. The strain is slightly reduced when using higher silver nanoparticles contents and the strain–stress behavior is quite similar to the multilayer reference film. The mechanical properties for these films are shown in Table I. The strain–stress values at break for the reference multilayer film were 460%–27 MPa. The values for the laminated sample at 1.0 wt % Ag were 445%–24 MPa. Those for the cast samples at 0.6 and at 1.0 wt % Ag were 495%–25.5 MPa and 450%–23 MPa, respectively. And, those for the sprayed samples at 0.6 and at 1.0 wt % Ag were 480%–26 MPa and 465%–24 MPa. Because the maximum difference in stress from the reference film is of only around 14% and the maximum difference in strain is only near 8%, these lie within the experimental error, as shown in Table I. This suggests that the deposited thin layer of nanocomposite has a minimum effect on the mechanical properties of the multilayer film.

**TABLE I**
**Mechanical Properties of Multilayer Films**

| Sample | Tensile strength (MPa) | Strain (%) |
|---|---|---|
| Reference multilayer film | 27 ± 5 | 460 ± 10 |
| Laminated film, 1.0 wt % Ag | 24 ± 4 (−11%) | 445 ± 11 (−3.2%) |
| Cast film, 0.6 wt % Ag | 25.5 ± 6 (−5.5%) | 495 ± 7 (+7.6%) |
| Cast film, 1.0 wt % Ag | 23 ± 6 (−14%) | 450 ± 9 (−2.1%) |
| Sprayed film, 0.6 wt % Ag | 26 ± 7 (−3.7%) | 480 ± 8 (+4.3) |
| Sprayed film, 1.0 wt % Ag | 24 ± 6 (−11%) | 465 ± 10 (+1%) |

In some applications, like in food packaging and medical applications, permeability to water vapor and gases, particularly oxygen, is critical to the protective properties of the plastic film. Varied permeabilities are also desired in certain applications like modified atmosphere packaging. Water vapor transmission rate (WVTR) and oxygen transmission rate (OTR) values obtained for the multilayer films are presented in Table II.

OTR of the multilayer films with the thin silver nanocomposite layer shows an increase with respect to the reference film. It can be observed that this increase is more significant for the cast (45%) and sprayed (50%) samples, and in all cases, there is a small increase in the oxygen transmission with the silver content. This could be related to the micro voids observed for the cast and sprayed samples by SEM analysis and to the lack of interactions between the PE chains and the silver aggregates that might lead to the formation of even more pronounced voids in the structure, which would boost the gas diffusivity.

**TABLE II**
**Oxygen Permeability and Water Vapor Transmission Results for the Multilayer Films**

| Sample | Oxygen permeability, 25°C ($cm^3\ m^{-2}\ d^{-1}$) | $H_2O$ vapor transmission rate, 38°C, 90% RH ($g\ m^{-2}\ d^{-1}$) |
|---|---|---|
| Reference multilayer film | 30 ± 0.7 | 6.0 ± 0.3 |
| Laminated film, 0.6 wt % Ag | 33 ± 0.3 (+10%) | 3.2 ± 0.4 (−46%) |
| Laminated film, 1.0 wt % Ag | 34 ± 0.2 (+13%) | 3.5 ± 0.6 (−41%) |
| Cast film, 0.6 wt % Ag | 41.5 ± 0.5 (+38%) | 4.3 ± 0.5 (−28%) |
| Cast film, 1.0 wt % Ag | 43.5 ± 1 (+45%) | 4.8 ± 0.6 (−20%) |
| Sprayed film, 0.6 wt % Ag | 42.5 ± 0.5 (+42%) | 5.4 ± 0.4 (−10%) |
| Sprayed film, 1.0 wt % Ag | 45.0 ± 0.2 (+50%) | 5.6 ± 0.2 (−7%) |

**TABLE III**
**Optical Properties of Multilayer Films**

| Sample | Transmittance (%) | Haze (%) |
|---|---|---|
| Reference multilayer film | 92.0 ± 0.2 | 10.6 ± 0.1 |
| Laminated film, 1.0 wt % Ag | 91.0 ± 0.3 (−1%) | 11.9 ± 0.4 (+12%) |
| Cast film, 1.0 wt % Ag | 88.5 ± 0.4 (−3.8%) | 13.8 ± 0.5 (+30%) |
| Sprayed film, 0.6 wt % Ag | 91.5 ± 0.1 (−0.5%) | 11.3 ± 0.7 (+6.6%) |
| Sprayed film, 1.0 wt % Ag | 89.5 ± 0.3 (−2.7%) | 12.7 ± 0.3 (+19%) |

The WVTR of the multilayer films with the silver nanocomposite layer shows a reduction with respect to the reference film. It can be seen that this reduction is more significant for the laminated samples (46%) in which no micro voids were seen by SEM. The reduction in WVTR could be related to the increase in the thickness of the PE layer, which is a barrier to water vapor. The difference observed between the different applications methods could be related to the voids observed in the casting and spraying methods (confirmed by SEM) that would have permitted the entry of more water molecules into the composites and have led to an increase in the WVTR values.

The optical properties, e.g., percent transmittance and haze, of the laminated, cast, and sprayed multilayer films are reported in Table III. The percent transmittance of multilayer films decreased from 92 to 88% with the incorporation of the silver-PE nanocomposite layer. It is also observed that the haze values lie in the range of 11.9–13.8 for films incorporating the silver nanocomposite layer. The increase in haze after incorporation of nanocomposite layer may be due to the scattering of light by the silver nanoparticles and aggregates.[47]

Figure 6(a–c) shows the antibacterial effect, in media broth, for 24 h, of multilayer films with the silver-PE nanocomposite applied using the three different methods. In all these figures, a typical behavior of bacterial growth with time can be observed. It can also be seen that at cero time, which corresponds to the moment the first biomass determination was carried out, which was in time performed 10 min after the sample preparation, all the silver-treated films show less biomass content than the control and reference samples, specially the films whose silver nanocomposite layers were deposited by casting and spraying, which could be related with a fast initial antimicrobial effect of the silver against this bacteria. Figure 6(a) corresponds to the sample where the silver nanocomposite layer was laminated, in which the number of *P. oleovorans* cells

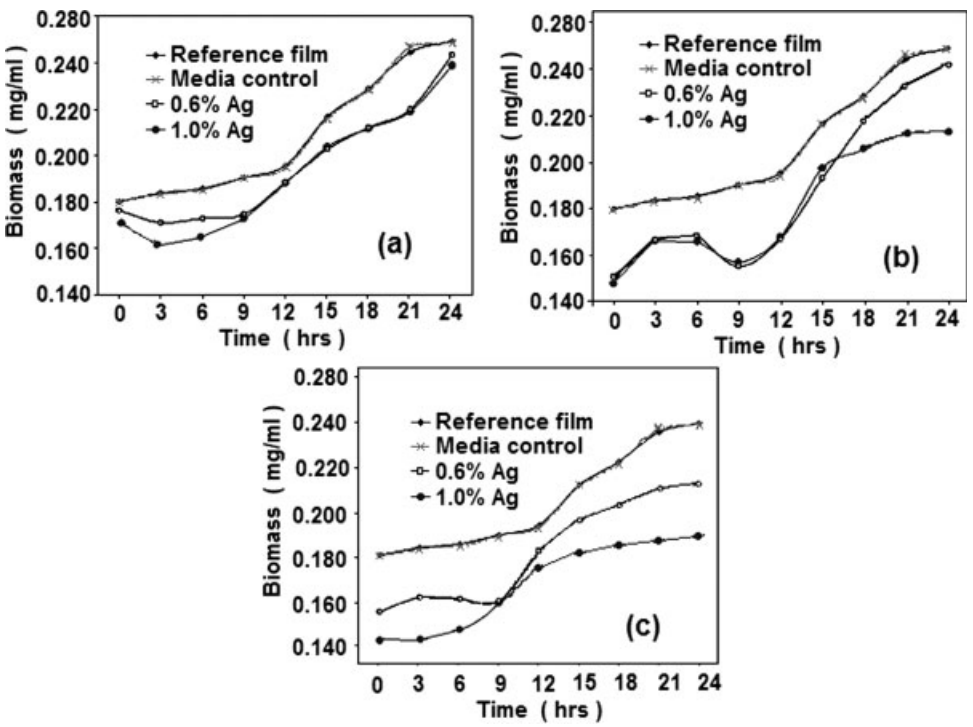


**Figure 6** Count of bacteria as biomass (mg/mL) versus time (h), expressing the antibacterial effect of multilayered films with the different silver nanocomposite application methods: (a) laminating, (b) casting, (c) spraying.

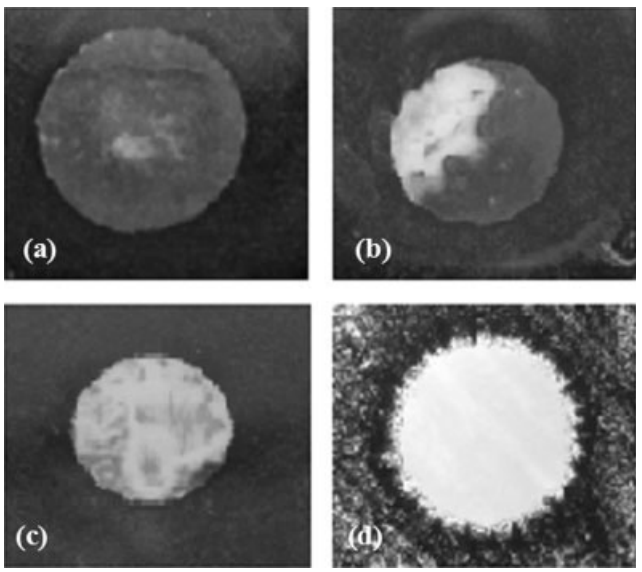


**Figure 7** Photographic image of the incubation of fungus *A. Níger*, after 72 h on: (a) reference multilayer film and different methods: (b) laminating, (c) casting, (d) spraying.

was reduced in the films with silver nanoparticles compared with the control and reference film for all the considered times. At the initial stage, 0–9 h, the number of *P. oleovorans* cells was reduced in the samples with higher silver content. After 24 h of exposition, the number of cells is quite similar for both silver contents and is very close to the media and reference film, reaching only a slight reduction on bacteria growth of around 10%.

Figure 6(b) shows the antibacterial effect of the sample where the silver nanocomposite layer was cast deposited. The number of *P. oleovorans* cells was reduced in the films with silver nanoparticles compared with the control and reference film for all the considered times. At the initial stage, 0–15 h, the number of bacteria cells was lower in the samples with both silver contents, and this reduction was more noticeable than in the samples prepared by lamination. After 24 h of exposition, the number of cells was lower for the higher silver content sample, reaching a reduction on bacteria growth of around 20%, whereas the lower silver content sample of 0.6% was very close to the media and reference film.

Figure 6(c) shows the antibacterial effect of the sample where the silver nanocomposite layer was sprayed, in which the number of bacteria cells at the initial stages is more significantly reduced for both silver contents, and after 24 h of exposition, the number of bacteria cells is lower than the media and reference film samples for both silver contents. It can be observed that at higher silver content, a reduction on bacteria growth of near 30% was achieved.

We can see that all three silver nanocomposite layer application methods exhibited a reduction in the biomasss production against the *P. oleovorans*, which was of around 30% with the higher silver nanoparticle concentration. We can infer that the spraying method would provide superior antibacterial properties, which could be related to the more visible nanoparticles and more visible voids on the surface of the films, as was confirmed by SEM, which may facilitate the diffusion and migration of the chemical entities such as water or silver ions within the matrix. This finding is in good accord with the experimental results obtained by other authors.[48] However, the low reduction on bacteria growth obtained in this work, when compared with the reported results,[39] suggests that these films are only partially effective in controlling the bacteria growth, at least with this type of bacteria.

Figure 7(a–d) shows the photographs of the incubation of fungus *A. Níger*, after 72 h, on the multilayer films with the three different silver nanocomposite application methods. It can be observed that fungi cover the reference multilayer film [Fig. 7(a)]. In the laminating method, Figure 7(b), a slight reduction in the fungus content can be observed, and in the casting method [Fig. 7(c)], an even greater reduction in the fungus content can be observed. However, in the spraying method, [Fig. 7(d)], a significant reduction in fungi growth can be observed. This again suggests that the spraying method was more efficient in fungus control and exhibit enhanced antifungal properties.

Figure 8 shows the percent reduction against the fungus *A. Níger* after 14 days, for the three multilayer samples with the silver nanocomposite layer and the reference, which was a silver nanoparticles water suspension, all at 1.0 wt % of silver content.

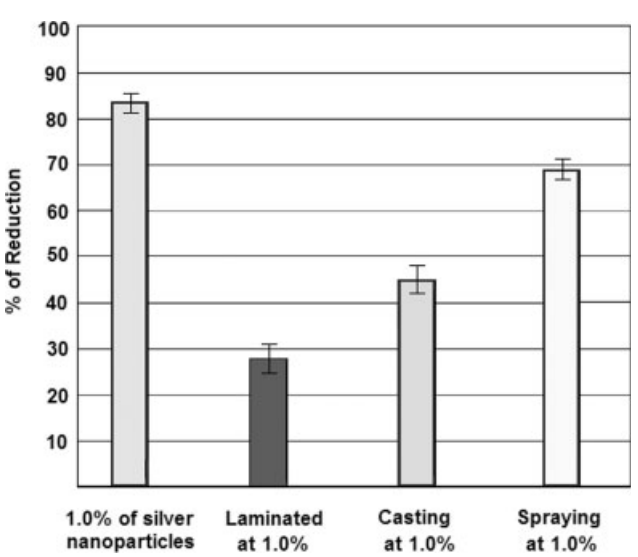


**Figure 8** Percent reduction against fungus *A. Níger* of solution analytes of the silver nanoparticles and multilayer film samples, collected after 14 days.

The measurements were performed with analytes collected after maintaining the samples in deionized water for 14 days, with continuous shaking. It can be seen that after 14 days, the biocide effect of the samples is maintained. The silver nanoparticles suspension, as expected, provided the highest percent reduction, above 80%, and the spraying method seemed to be the best for applying the silver nanocomposite layer and attaining the higher percent of growth reduction against *A. niger*. These results suggest that these films show a better biocide effect against the fungus than against the bacteria, which may be related to the different effect of the silver nanoparticles on different types of micro organisms, which has been reported by other authors.[31,49]

The antimicrobial activity of silver is dependent on the silver cation $Ag^+$, which strongly binds to electron donor groups in biological molecules containing sulfur, oxygen, or nitrogen. The biological performance of silver ions is dose-dependent. Low concentrations <35 ppb are mainly bactericide, whereas higher doses can be toxic to human cells, ranging from low or high local toxicity to systemic effects like argyria in high doses (>4–6 g total silver content in the body).[36] Hence, the silver-based antimicrobial materials have to release $Ag^+$ ions to be effective. Figure 9 shows the characteristic nature of the nanocomposite samples as a silver ion emitter in an aqueous environment. These measurements were performed with analytes collected at different times of continuous shaking in deionized water, similar to the procedure described earlier. From this figure, it can be concluded that the samples are releasing the $Ag^+$ biocide and that its release increases with time. However, the increase is found to be more significant at higher times and the difference between 3 and 7 days is less notable compared with the difference observed between 7 and 14 days. It can be seen that the silver nanoparticles suspension, as expected, is the one with the highest $Ag^+$ release, and that the spraying method, used for applying the silver nanocomposite layer, is the one that produces the highest $Ag^+$ release. Even though we did not considered determinations at exposure times longer than 14 days, we believe that these films will continue to release silver ions, according with the similar results reported by other authors.[37] It can be seen that there is a good agreement between the ion release content and the fungicidal test results. In addition, these results are in good agreement with the experimental results from other authors.[37,48] To explain the differences observed in the method of silver nanocomposite application, we suggests that the rate of diffusion is increased in the samples with tiny voids, which facilitate the penetration of humidity throughout this layer, and as a consequence, the migration of silver ions and increases the rate of $Ag^+$ release.

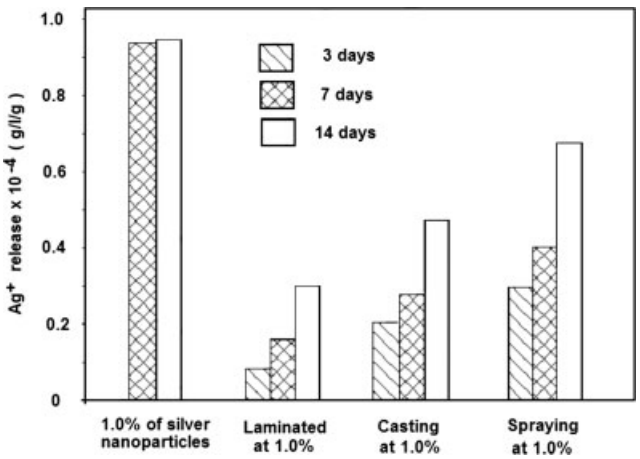


**Figure 9** Silver ion release as a function of immersion time for solution analytes of the silver nanoparticles and different multilayer samples.

As was seen by SEM, the samples with a sliver nanocomposite layer deposited by lamination are highly smooth with no apparent voids on its surface, and because PE is a nonhygroscopic polymer, there will be much lower water diffusion through the polymer matrix. On the other hand, the samples in which the layer was deposited by casting have some visible voids, and the sample deposited by spraying has even more noticeable voids that would facilitate the diffusion of water and silver and enhance the biocide properties.

The microorganism's strains used in our test system showed different sensitivities to silver ions. Mechanistically, the mode of action at low silver concentrations is an interference of $Ag^+$ with the murein of the bacterial cell wall.[38] Differences in sensitivity are therefore very likely dependent on the type of bacteria and the type of fungus.

## CONCLUSIONS

The effect of a silver nanoparticles layer and the method of deposition on the mechanical, barrier, optical, and biocide properties of multilayered films were investigated. From TEM images, we determined that the average silver particle size after an ultrasonic irradiation process was around 26 nm. It was found that the casting and spraying methods used to apply the silver nanocomposite layer show tiny pores on the surface that could increase the rate of diffusion of chemical entities, such as water, gas, and silver ions, into the composites and enhance the microbial activity of the silver particles. The thin layer of nanocomposite has only a minimum effect on the mechanical and optical properties of the multilayer film. It was found that a superior effect of these films on fungus control than their effect on

bacteria growth control. The spraying method showed superior biocide properties to control the growth of the bacteria *P. oleovorans* and the fungus *A. Níger*. This biocide effect is maintained even after 14 days of exposure. The antimicrobial properties were enhanced in the samples with tiny voids, which facilitate the migration of silver ions and increase the rate of $Ag^{+}$ release. A good agreement was found between the ion release experiments and antimicrobial test results.

R. Guedea-Miranda wishes to thank CONACYT for granting him a scholarship to carry out his MSc. Finally, the authors thank to M. L. Lopez-Quintanilla, M. C. Gonzalez-Cantu, M. Sanchez-Adame, J. A. Sanchez-Molina, J. Borjas-Ramos, J. A. Espinoza-Muñoz, J. Zamora, B. Huerta-Martinez, M. Lozano, R. Cedillo, and J. Rodríguez-Velázquez for their assistance in the sample preparation and characterization.

## References

1. Ming, J.; Chen, Ch.; Huang, Ch.; Chang, F.; Chen, S.; Su, P. K. Ch.; Hsu, J.; Chen, B.; Yu, Y. J Appl Polym Sci 2006, 99, 1576.
2. Yeh, J.; Liou, S.; Lin, C.; Wu, P.; Tsai, T. Chem Mater 2001, 13, 1131.
3. Valdes, S. S.; Quintanilla, M. L.; Vargas, E. R.; Rodrıiguez, F. M.; Rodriguez, J. G. Macromol Mater Eng 2006, 291, 128.
4. Zanetti, M.; Lomakin, S.; Camino, G. Macromol Mater Eng 2000, 279, 1.
5. Zong, R.; Hu, Y.; Wang, S.; Song, L. Polym Degrad Stab 2004, 83, 423.
6. Binder, S.; Levitt, A. M.; Sacks, J. J.; Hughes, J. M. Science 1999, 284, 1311.
7. Wendt, C.; Wiesenthal, B.; Dietz, E.; Ruden, H. J Clin Microbiol 1998, 36, 3734.
8. Neely, A. N.; Maley, M. P. J Clin Microbiol 2000, 38, 724.
9. Lin, J.; Tiller, J. C.; Lee, S. B.; Lewis, K.; Klivanov, A. M. Biotechnol Lett 2002, 24, 801.
10. Sauvet, G.; Fortuniak, W.; Kazmierski, K.; Chojnowski, J. J Polym Sci Part A: Polym Chem 2003, 41, 2939.
11. Patel, S. A.; Patel, M. V.; Ray, A.; Patel, R. M. J Polym Sci Part A: Polym Chem 2003, 41, 2335.
12. Kanazawa, A.; Ikeda, T.; Endo, T. J Polym Sci Part A: Polym Chem 1994, 32, 1997.
13. Arnt, L.; Nuesslein, K.; Tew, G. N. J Polym Sci Part A: Polym Chem 2004, 42, 3860.
14. Sun, Y.; Sun, G. Macromolecules 2002, 35, 8909.
15. Sun, Y.; Sun, G. J Appl Polym Sci 2001, 81, 617.
16. Braun, M.; Sun, Y. J Polym Sci Part A: Polym Chem 2004, 42, 3818.
17. Sondi, I.; Salopek-Sondi, B. J Colloid Interface Sci 2004, 275, 177.
18. Alt, V.; Bechert, T.; Steinrucke, P.; Wagener, M.; Seidel, P.; Dingeldein, E.; Domann, E.; Schnettler, R. Biomaterials 2004, 25, 4383.
19. Jiang, H.; Manolache, S.; Wong, A. L.; Denes, F. S. J Appl Polym Sci 2004, 93, 1411.
20. Klueh, U.; Wagner, V.; Kelly, S.; Johnson, A.; Bryers, J. D. J Biomed Mater Res 2000, 53, 621.
21. Son, W. K.; Youk, J. H.; Lee, T. S.; Park, W. H. Macromol Rapid Commun 2004, 25, 1632.
22. Silver, S. FEMS Microbiol Rev 2003, 27, 341.
23. Wassall, M. A.; Santin, M.; Isalberti, C.; Cannas, M.; Denyer, S. P. J Biomed Mater Res 1997, 36, 325.
24. Blaker, J. J.; Nazhat, S. N.; Boccaccini, A. R. Biomaterials 2004, 25, 1319.
25. Wohrmann, R. M. J.; Hentschel, T.; Munstedt, H. Adv Eng Mater 2000, 2, 380.
26. Appendini, P.; Hotchkiss, J. H. Innovat Food Sci Emerg Technol 2002, 3, 113.
27. Gupta, A.; Silver, S. Nat Biotechnol 1998, 16, 888.
28. Feng, Q. L. J Biomed Mater Res 2000, 52, 662.
29. Matsumura, Y. Appl Environ Microbiol 2003, 69, 4278.
30. Gupta, A.; Maynes, M.; Silver, S. Appl Environ Microbiol 1998, 64, 5042.
31. Grier, N. In Disinfectants, Sterilization and Preservations, 3rd ed.; Block, S., Ed.; Lea & Febiger: Philadelphia, 1983, p 141.
32. Trevors, J. T. Water Air Soil Pollut 1987, 34, 409.
33. Shearer, A. E. H.; Paik, J. S.; Hoover, D. G.; Haynie, S. L.; Kelly, M. J. Biotechnol Bioeng 2000, 67, 141.
34. Nover, L.; Scharf, K. D.; Neumann, D. Mol Cell Biol 1983, 3, 1648.
35. Fornes, T. D.; Paul, D. R. Polymer 2003, 44, 3945.
36. Gosheger, G.; Hardes, J.; Ahrens, H.; Streitburger, A.; Buerger, H.; Erren, M.; Gunsel, A.; Kemper, F. H.; Winkelmann, W.; von Eiff, C. Biomaterials 2004, 25, 5547.
37. Jeong, S. H.; Hwang, Y. H.; Yi, S. C. J Mater Sci 2005, 40, 5413.
38. Fu, J.; Ji, J.; Fan, D.; Shen, J. J Biomed Mater Res A 2006, 79, 665.
39. Ewald, A.; Glückermann, S. K.; Thull, R.; Gbureck, U. Biomed Eng Online 2006, 5, 1186.
40. Chen, Y.; Li, H. J Appl Polym Sci 2005, 97, 1553.
41. Feng, W.; Isayev, A. I. Polymer 2004, 45, 1207.
42. Jianling, Z.; Zhimin, L.; Buxing, H.; Tao, J.; Weise, W.; Jing, C. J Phys Chem B 2004, 108, 2200.
43. Gul, R. J.; Wan, P. S.; Hyungsu, K.; Wook, L. J. Mater Sci Eng C 2004, 24, 285.
44. Lee, E. C.; Mielewski, D. F.; Baird, R. J Polym Eng Sci 2004, 44, 1773.
45. Brause, R.; Moeltgen, H.; Kleinermanns, K. Appl Phys B: Lasers Opt 2002, 75, 711.
46. Sosa, I. O.; Noguez, C.; Barrera, R. G. J Phys Chem B 2003, 107, 6269.
47. Ghosh, K.; Maiti, S. N. J Appl Polym Sci 1996, 60, 323.
48. Kumar, R.; Howdle, S.; Munstedt, H. J Biomed Mater Res Part B: Appl Biomater 2005, 75, 311.
49. Morones, J.; Elechiguerra, J.; Camacho, A.; Holt, K.; Kouri, J.; Ramirez, J. T.; Yacaman, M. Nanotechnology 2005, 16, 2346.